



**HAL**  
open science

## Seasonal variation of equatorial wave momentum fluxes at Gadanki ( $13.5^\circ$ N, $79.2^\circ$ E)

M. N. Sasi, V. Deepa

► **To cite this version:**

M. N. Sasi, V. Deepa. Seasonal variation of equatorial wave momentum fluxes at Gadanki ( $13.5^\circ$  N,  $79.2^\circ$  E). *Annales Geophysicae*, 2001, 19 (8), pp.985-990. hal-00316891

**HAL Id: hal-00316891**

**<https://hal.science/hal-00316891>**

Submitted on 18 Jun 2008

**HAL** is a multi-disciplinary open access archive for the deposit and dissemination of scientific research documents, whether they are published or not. The documents may come from teaching and research institutions in France or abroad, or from public or private research centers.

L'archive ouverte pluridisciplinaire **HAL**, est destinée au dépôt et à la diffusion de documents scientifiques de niveau recherche, publiés ou non, émanant des établissements d'enseignement et de recherche français ou étrangers, des laboratoires publics ou privés.

## Seasonal variation of equatorial wave momentum fluxes at Gadanki (13.5° N, 79.2° E)

M. N. Sasi and V. Deepa

Space Physics Laboratory Vikram Sarabhai Space Centre Trivandrum-695022, India

Received: 6 November 2000 – Revised: 14 March 2001 – Accepted: 15 March 2001

### Abstract.

The vertical flux of the horizontal momentum associated with the equatorial Kelvin and Rossby-gravity waves are estimated from the winds measured by the Indian MST radar located at Gadanki (13.5° N, 79.2° E) during September 1995 to August 1996 in the tropospheric and lower stratospheric regions for all four seasons. The present study shows that momentum flux values are greater during equinox seasons than solstices, with values near the tropopause level being  $16 \times 10^{-3}$ ,  $7.4 \times 10^{-3}$ ,  $27 \times 10^{-3}$  and  $5.5 \times 10^{-3} \text{ m}^2 \text{ s}^{-2}$  for Kelvin waves and  $5.5 \times 10^{-3}$ ,  $3.5 \times 10^{-3}$ ,  $6.7 \times 10^{-3}$  and  $2.1 \times 10^{-3} \text{ m}^2 \text{ s}^{-2}$  for RG waves during autumnal equinox, winter, vernal equinox and summer seasons, respectively. Using these momentum flux values near the tropopause level, acceleration of the mean flow in the stratosphere up to a 29 km height were computed following Plumb (1984), by considering the wave-meanflow interaction and the deposition of the momentum through the radiative dissipation of the waves. A comparison of the estimated mean-flow acceleration in the stratosphere compares well, except at a few height levels, with the observed mean-flow accelerations in the stratosphere derived from the radiosonde data from a nearby station.

**Key words.** Meteorology and atmospheric dynamics (tropical meteorology; waves and tides)

### 1 Introduction

The quasi-biennial oscillations (QBO) dominate the dynamics of the equatorial lower stratosphere. The basic mechanism responsible for the QBO is the wave-meanflow interaction, wherein upward propagating equatorial waves, i.e. Kelvin and Rossby-gravity (RG) waves interact with the stratospheric meanflow and deposit their momentum producing alternating westerly and easterly regimes, respectively. An important parameter used in the simulation of the QBO

is the prescription of the meridionally averaged vertical flux of the horizontal momentum,  $\overline{u'w'}$  ( $u'$  and  $w'$  are perturbations in the zonal and vertical velocity) of the Kelvin and RG waves at the lower boundary (at a height of  $\sim 17$  km) of the model (e.g. Holton and Lindzen, 1972). The QBO is sensitive to any change in the wave momentum flux. The QBO period decreases with an increase in wave momentum fluxes at the lower boundary (Plumb, 1977). In a numerical simulation of QBO, Dunkerton (1981) has shown that the period of the QBO increased by 22% when the RG wave flux was reduced by a factor of 2. Geller et al. (1997) have shown that the QBO period changed from  $\sim 25$  months to  $\sim 45$  months when the Kelvin and RG wave momentum fluxes were changed from  $\pm 8 \times 10^{-3} \text{ m}^2 \text{ s}^{-2}$  to  $\pm 2 \times 10^{-3} \text{ m}^2 \text{ s}^{-2}$ ; the QBO period of  $\sim 33$  months corresponds to a flux value of  $\pm 4 \times 10^{-3} \text{ m}^2 \text{ s}^{-2}$ . These studies show the importance of an observational study of the momentum fluxes of equatorial waves, which are driving the QBO oscillations in the equatorial lower stratospheric zonal winds. The variations in the flux values of the equatorial waves change the forcing of the stratospheric mean zonal wind, which ultimately changes the QBO period. Thus, the study of the variation of flux values is important for the simulation of QBO. One of the earliest estimates of momentum fluxes associated with the equatorial waves was done using radiosonde temperature and zonal wind data by Wallace and Kousky (1968). Since then many more similar studies have been made by others using radiosonde data. Recently, using radiosonde data, Sato and Dunkerton (1997) have estimated the momentum fluxes associated with the equatorial waves. With the advent of MST radar, which can measure wind components with fine vertical resolution, the momentum fluxes can be estimated directly from the vertical and zonal components of the wind (Sasi et al., 1999).

Equatorial wave momentum fluxes during different seasons in the lower atmosphere over the tropical station Gadanki are estimated, using a method developed by Sasi et al. (1999) from winds measured by the Indian MST radar and the results are presented in this paper. These flux values are used to simulate the meanflow acceleration in the

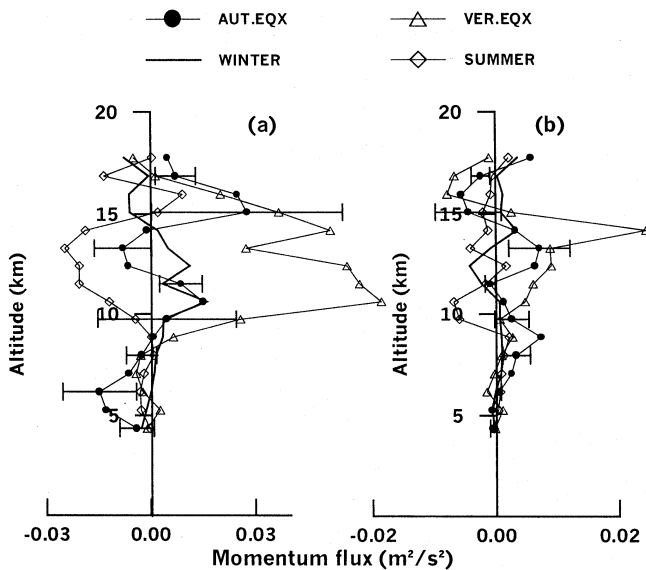


**Fig. 1.** Height profile of the vertical flux of the zonal momentum,  $\overline{u'w'}$  over Gadanki during the different seasons (a) Kelvin wave (b) RG wave. Filled circles, continuous line, triangles and squares represent momentum fluxes for the autumnal equinox, winter, vernal equinox and summer seasons, respectively. Horizontal bars show dispersion of  $\overline{u'w'}$  for the autumn equinox season.

stratosphere up to a 30 km height level. For this purpose, the method outlined by Plumb (1984) is used. The meanflow accelerations are also calculated using monthly mean winds obtained from balloon data from a nearby station and are then compared with the simulated ones during different seasons. Section 2 briefly describes the data used for the present study and the method used to derive the momentum fluxes from the radar wind data. Seasonal variation of observed momentum fluxes are described in Sect. 3. The mean-flow accelerations in the stratosphere produced by the radiative dissipation of equatorial Kelvin and RG waves are simulated using the observed momentum fluxes near the tropopause level and these are presented in Sect. 4. Summary and conclusions are included in Sect. 5.

## 2 Data and method of analysis

For the present study, daily wind data collected from the Indian MST radar located at Gadanki (13.5° N, 79.2° E) are used. The data were collected for the period September 1995 to August 1996, covering four seasons. Daily Doppler spectra corresponding to the six beams (two zenith beams and four oblique beams in the north, south, east and west directions) with a vertical resolution of 150 m were first converted to line-of-sight (LOS) wind profiles. From these daily vertical profiles of LOS winds corresponding to the six beams, the zonal ( $u$ ), meridional ( $v$ ) and vertical ( $w$ ) components of the daily winds were derived using a least-squares technique, assuming a vertical wind contribution to the LOS winds ob-

tained for the oblique beams (Sato, 1989). Once the vertical profiles (resolution of 150 m) of  $u$ ,  $v$ , and  $w$  are obtained, they are subjected to a 5-point running mean in height with weights 0.125, 0.125, 0.5, 0.125 and 0.125. This smoothing procedure will reduce the small scale wind fluctuations with height, which may be due to random fluctuations or real atmospheric phenomena. However, wave components for this study are the equatorial waves whose vertical wavelengths lie in the range of 4–12 km. The time series of  $u$  and  $w$  are obtained from height-smoothed wind profiles. There exists a few gaps in the time series which are filled by linear interpolation. The length of the time series in each season is 48 days. This data length is sufficient for the study of slow Kelvin (10–20 day period) and RG waves (3–5 day period).

For this study, the time series of zonal wind  $u$  and vertical wind  $w$  are used for identifying various equatorial wave modes and for computing the associated momentum fluxes. The method employed for this purpose is the same one used by Sasi et al. (1999), and is briefly described as follows. For Kelvin and RG waves, the perturbations  $u'$  and  $w'$  are in phase (time) at a particular height (Holton, 1980) and this property is reflected in the cross spectrum of  $u$  and  $w$ . First, the cross-spectra of  $u$  and  $w$  at suitable height intervals are found. Since  $u$  and  $w$  vary in a non-random manner for the equatorial waves, a high coherence value indicates the presence of wave motion corresponding to that frequency. The prominent periods with high coherence values corresponding to different wave modes present in the cross spectrum are delineated. Then the vertical coherence of the zonal wind is calculated to see whether these identified periods belong to any vertically propagating wave modes. For calculating vertical coherence, a reference height is chosen in the upper troposphere and the selection of the height is based on the high coherence (between  $u$  and  $w$ ) values. Then the cross spectrum of the zonal winds ( $u$ ) and the vertical coherence at all other heights relative to these heights were found. If the vertical coherence is also high for the prominent periods obtained in the cross spectrum, one can reasonably conclude that a high coherence between  $u$  and  $w$  is probably due to the propagation of atmospheric waves in the vertical direction. Once these periods are identified, the vertical propagation characteristics of the waves are estimated from the phase (time of maximum) profile of  $u$  corresponding to that particular period of the wave mode by Fourier analysis of the time series of  $u$  at different altitudes. Thus, the prominent periods and the corresponding vertical wavelengths determine the presence of different wave modes. The Kelvin and RG wave modes cannot be identified based on the periods and vertical wavelengths alone. Relatively small amplitude values of  $v$ , when compared to that of  $u$ , may indicate that they are perturbations produced by Kelvin waves and similarly oscillations produced by RG waves  $u$  and  $v$  will have comparable amplitudes. In this manner, 8–12 day oscillations were identified as Kelvin waves and 3–4 day oscillations as RG waves. Following this, the momentum fluxes  $\overline{u'w'}$  corresponding to these wave modes are calculated from the reconstructed time series of  $u$  and  $w$  for the particular periods from

the amplitudes and phases obtained from their Fourier spectra. The Kelvin wave periods for autumnal equinox, winter, vernal equinox and summer seasons are 12, 9.6, 8 and 9.6 days, respectively. For RG waves, the corresponding periods are 3.4, 4, 3.6 and 3.2 days, respectively

### 3 Seasonal variation of momentum flux values

The vertical profiles of the momentum flux  $\overline{u'w'}$  obtained for all four seasons for Kelvin waves and RG waves are shown in Fig. 1a and Fig. 1b, respectively. The variability of  $u'w'$  over the 48-day duration is computed from the deviations of  $u'w'$  from  $\overline{u'w'}$  and is represented by the r.m.s. deviation ( $\sigma$ ) and shown by horizontal bars at every 1.8 km height for the autumn equinox season. Similar  $\sigma$  values were estimated for other seasons as well, but are not shown. The estimated r.m.s. errors in  $\overline{u'w'}$  derived from the MST radar measured  $u$  and  $w$  components of the wind are  $1.2 \times 10^{-3} \text{m}^2 \text{s}^{-2}$  (Sasi et al., 1999) and at most of the altitudes, the r.m.s. deviations shown in Figs. 1a and b are also of the same order. It may be mentioned here that Sasi et al. (1999) estimated errors in  $\overline{u'w'}$  based on the measurement errors in  $u$  and  $w$ . In addition to these errors, geophysical noise present in the radar wind data produces statistical uncertainty in the estimated momentum flux values depending on the magnitude of the atmospheric momentum flux  $\langle u(t)w(t) \rangle$  relative to the geometric mean energy  $\sqrt{\langle u^2(t) \rangle \langle w^2(t) \rangle}$  (Kudeki and Franke, 1998). Accordingly, Kudeki and Franke suggest long integration times for statistically significant estimates of the momentum flux. Though the concept developed by them is primarily applicable to gravity wave momentum flux estimates (based on a particular spectral distribution of energy), the idea of using a long integration time is equally applicable for other wave motions, such as equatorial waves. A calculation of the ratio of momentum to the geometric mean energy in our case gives a value of  $\sim 10\%$  and we have used an integration time of 48 days, which may be sufficient for a statistically reliable estimate of the momentum flux. However, the estimated r.m.s. error in the momentum flux  $\overline{u'w'}$  given by Sasi et al. (1999) could be a lower limit in the context of possible errors introduced by geophysical noise.

A close examination of Figs. 1a and b shows that momentum flux values have both positive and negative signs. Both coherence (between  $u'$  and  $w'$ ) and vertical coherence of  $u'$  show large values (above 0.9) in certain height ranges (especially above 10 km) and at these heights, the  $\overline{u'w'}$  are also positive. This is true for the autumn equinox, winter and vernal equinox seasons. But for the summer season at some of the heights where coherence is high, the momentum flux values are negative. The reason for this distinctly different behaviour during the summer season is not clear, although it is possible that this may be linked to a tropical easterly jet (TEJ) which is strongly present just below the tropopause height during this season.

From these figures, it is seen that the flux values for both Kelvin and RG waves obtained during the equinox seasons

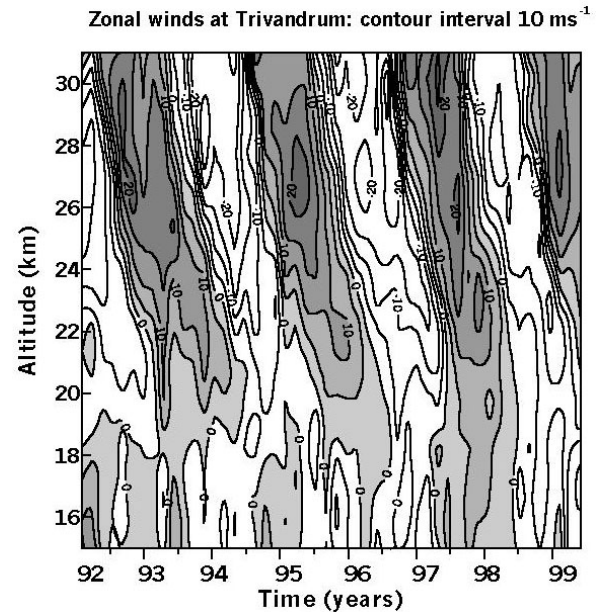


**Fig. 2.** Height-time structure of the zonal wind ( $u$ ) obtained from balloon data from Trivandrum ( $8.5^\circ \text{N}$ ,  $77^\circ \text{E}$ ) during 1992–1999. The westerly winds are shaded.

(especially during vernal equinox) are larger than those obtained during the solstice seasons. It may be mentioned here that a recent study by Wikle et al. (1997) shows that the equatorial wave activity in the upper troposphere and lower stratosphere over the tropical Pacific has a semiannual variation with peaks occurring in late winter-spring and late summer-fall. The equatorial waves are forced in the tropical troposphere as a response to the heating due to a large-scale cumulus convection. It is possible that the latent heat released within the Inter Tropical Convergence Zone (ITCZ) could act as a prominent source for equatorial waves. The large-scale convection and cyclonic vorticity associated with the ITCZ are, in general, favourable for the intensification of the waves. In its semiannual oscillation the ITCZ migrates farthest away from the equator into summer continental regions. During northern summer, the ITCZ is entirely in the northern hemisphere while during southern summer (northern winter) the ITCZ is located south of the equator. At the latitude of the Indian subcontinent ( $80^\circ \text{E}$ – $82.5^\circ \text{E}$ ), the seasonal migration of the ITCZ occurs between  $\sim 5^\circ \text{S}$  and  $\sim 20^\circ \text{N}$  (Srinivasan and Smith, 1996). The position of the ITCZ during the equinox seasons, on average, is centred approx. at  $10^\circ \text{N}$  latitude over the Indian subcontinent. One may reasonably expect during the equinox seasons that the equatorial wave excitation will be more efficient when the source is closer to the equator, especially over land and these waves may transfer more momentum during this time. Therefore, the momentum fluxes may be expected to be greater during the equinoxes than during the solstices. The present observation is consistent with this argument.

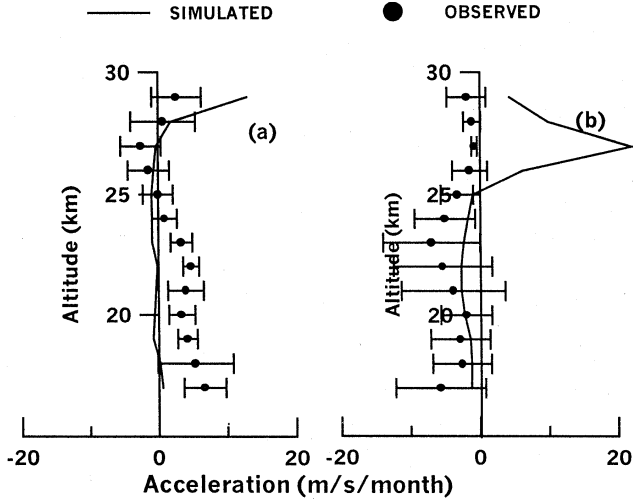


**Fig. 3.** Height profile of the zonal mean-flow acceleration in the stratosphere. Continuous line represents simulated profile (simulated using equatorial wave momentum fluxes near the tropopause level over Gadanki) and filled circles represent the observed profile (from balloon data over Trivandrum). Horizontal bars show r.m.s. variation of the observed zonal wind acceleration, (a) autumnal equinox (b) vernal equinox.

The average observed momentum flux values near the tropopause height for Kelvin waves are  $16 \times 10^{-3}$ ,  $7.4 \times 10^{-3}$ ,  $27 \times 10^{-3}$  and  $5.5 \times 10^{-3} \text{ m}^2 \text{ s}^{-2}$  during the autumn equinox, winter, vernal equinox and summer seasons, respectively. The corresponding values for RG waves are  $5.5 \times 10^{-3}$ ,  $3.5 \times 10^{-3}$ ,  $6.7 \times 10^{-3}$  and  $2.1 \times 10^{-3} \text{ m}^2 \text{ s}^{-2}$ , respectively. It may be interesting to compare these values with those obtained from rawinsonde data at Singapore by Sato and Dunkerton (1997). They obtained a value of  $2 - 9 \times 10^{-3} \text{ m}^2 \text{ s}^{-2}$  for Kelvin wave momentum fluxes and  $0.4 \times 10^{-3} \text{ m}^2 \text{ s}^{-2}$  for RG waves using a direct method (from the quadrature spectra of temperature and zonal components of the winds).

#### 4 Simulation of mean-flow acceleration

With the observed momentum flux values of the Kelvin and RG waves near the tropopause level, it is possible to estimate the acceleration of the mean-flow in the stratosphere, which is induced by the radiative dissipation of these waves. For this purpose, the method outlined by Plumb (1984) is used. The momentum flux associated with each wave mode can be expressed as

$$\rho(z)\overline{u'w'}(z) = \rho(z_0)\overline{u'w'} \exp\left(-\int_{z_0}^z g_i(z)dz\right) \quad (1)$$

where  $\rho(z_0)\overline{u'w'}$  is the momentum flux at the tropopause height,  $z_0 = 17 \text{ km}$  and  $g_i$ s are given by

$$g_k(z) = \frac{N\alpha}{k_K(\overline{U} - c_K)^2} \quad (2)$$

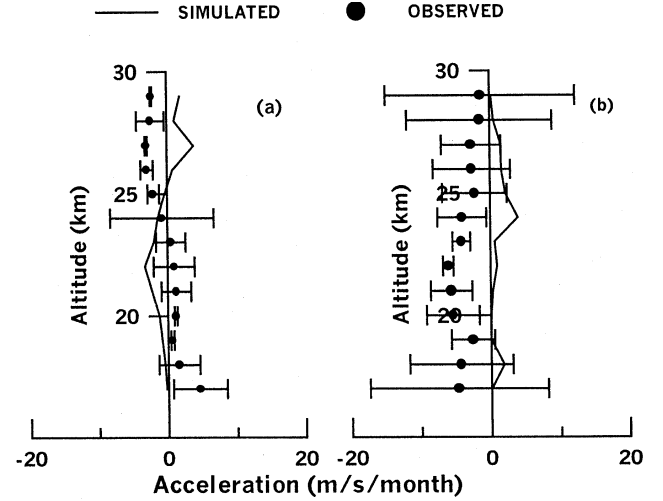


**Fig. 4.** Same as Fig. 3 but for (a) winter (b) summer

for Kelvin waves and

$$g_{RG}(z) = \frac{N\alpha}{k_{RG}(\overline{U} - c_{RG})^2} \left( \frac{2\beta}{k_{RG}^2(\overline{U} - c_{RG})} - 1 \right) \quad (3)$$

for RG waves.

The notations used are:  $N$  = Brunt-Vaisala frequency,  $\alpha$  = Newtonian cooling coefficient,  $\beta = 2\Omega/a_0$   $\Omega$  = angular velocity of earth's rotation,  $a_0$  = radius of the earth,  $k_K$  = zonal wavenumber of the Kelvin wave,  $k_{RG}$  = zonal wavenumber of the RG wave,  $c_K$  = zonal phase speed of the Kelvin wave,  $c_{RG}$  = zonal phase speed of the RG waves,  $z$  = altitude,  $z_0$  = reference altitude (17 km). The values of these parameters are taken from Plumb (1984). The values of atmospheric density  $\rho$  were taken from the reference atmospheric model by Sasi and Sengupta (1979). The Brunt Vaisala frequency is calculated using the formula

$$N^2 = \frac{g}{T} \left( \frac{dT}{dz} + \frac{g}{c_p} \right) \quad (4)$$

where  $g$  is the acceleration due to gravity,  $T$  is the temperature and  $c_p$  is the specific heat of air at constant pressure. For calculating  $N^2$ , the temperature profile obtained from high altitude balloon data from a nearby station at Trivandrum ( $8.5^\circ \text{ N}$ ,  $77^\circ \text{ E}$ ) are used. These high altitude balloons are flown every Wednesday to measure the temperature and the winds up to approx. a 35 km height. The mean zonal winds  $\overline{U}$  were also obtained from the same balloon data and were used in Eqs. (2) and (3). Both  $\overline{U}$  and  $N^2$  correspond to the same period as the radar observations covering the different seasons.

Equation (1) gives the vertical profile of the momentum flux values above 17 km. The flux convergence produced by

the damping of the waves is

$$\frac{\partial}{\partial z} \rho(z) \overline{u'w'}(z) = -\rho(z_0) u'w'(z_0) g_i(z) \times \exp\left(-\int_{z_0}^z g_i(z) dz\right) \quad (5)$$

and the mean-flow acceleration  $\frac{\partial \overline{U}}{\partial t}$  caused by the above convergence is calculated from

$$\frac{\partial \overline{U}}{\partial t} = \frac{1}{\rho(z)} \frac{\partial \rho(z) \overline{u'w'}(z)}{\partial z} \quad (6)$$

The mean-flow acceleration as obtained from equation (6) is calculated for all four seasons during the year 1995–1996.

Figure 2 gives the time-height cross section of the monthly mean zonal winds in the 15–31 km height over the Trivandrum region for the 1992–1999 period. The QBO can be clearly seen for  $\sim 3$  cycles in this figure. During the period of the MST radar observation (September 1995 to August 1996), the stratospheric zonal winds are in the process of changing from a westerly to easterly regime at lower altitudes and they are easterly at higher altitudes. The zonal wind accelerations in the different seasons during 1995–1996 in the 18–29 km height range were calculated from the observed zonal winds over Trivandrum. These mean-flow accelerations (both observed from the balloon data and simulated using equatorial wave momentum fluxes at the tropopause level) during the equinoxes and the solstices are shown in Fig. 3 and Fig. 4, respectively. The continuous curve represents the simulated value and the filled circles represent the observed value. The r.m.s. variations ( $\sigma_a$ ) of the observed zonal wind acceleration at different levels are estimated and shown as horizontal bars at every 1 km height in the observed profile. It is seen from Fig. 3a that the observed and simulated accelerations during the autumn equinox season are agreeing with each other above 25 km, as the simulated accelerations are lying within  $\pm \sigma_a$  of the observed ones. Yet for the vernal equinox season, there is good agreement between the two below the 25 km height level (Fig. 3b). There is disagreement between the simulated and observed accelerations below 24 km during the autumn equinox. Above 25 km, during the vernal equinox seasons, the disagreement is stronger. During the winter season, there is hardly any agreement between the two (Fig. 4a). Probably among the four seasons, the simulated and observed accelerations during the summer show agreement in a larger height region, as can be seen in Fig. 4b; the disagreement is seen only between the 20 and 24 km heights. The differences seen between the observed and simulated zonal wind accelerations during the different seasons may be due to the role played by gravity waves in producing the meanflow acceleration. Recent studies show that gravity waves also play an important role in producing meanflow acceleration in the equatorial stratosphere (Dunkerton, 1997; Mayr et al., 1997) and inclusion of gravity waves along with the equatorial waves may produce more realistic simulated zonal wind accelerations in the low-latitude stratosphere.

## 5 Summary and conclusions

The seasonal variation of equatorial wave momentum fluxes in the troposphere and lower stratosphere over Gadanki (13.5° N, 79.2° E) is studied using MST radar wind data for one year from September 1995 to August 1996. It is observed that the momentum flux values in the upper troposphere are at a maximum during both the autumnal and vernal equinox periods and at a minimum during both the summer and winter solstices. This is true for both Kelvin and RG waves. One of the sources that forces the equatorial waves could be the ITCZ. The observed seasonal variation of the equatorial wave momentum fluxes may be related to the semiannual meridional migration of the ITCZ.

Mean-flow accelerations at every 1 km are calculated for the 17–29 km region using balloon data (zonal wind) over Trivandrum (8.5° N, 77° E), a station lying close to Gadanki, for the 1995–1996 period and are compared with simulated ones obtained using the observed (from the MST radar) momentum flux values at the tropopause level for the different seasons. Though the simulated and observed mean-flow acceleration at the stratospheric levels, in general, agree with each other, in certain height regions, significant differences between the two are seen. These differences may be due to the role played by gravity waves in producing the mean-flow acceleration in the low-latitude stratosphere.

*Acknowledgements.* The National MST Radar Facility (NMRF) is operated as an autonomous facility under DOS with partial support from CSIR. The authors are very thankful to the scientists and engineers from NMRF for making the equatorial wave experiment a success. One author (V D) is thankful to the ISRO for providing Research Fellowship. Very useful and constructive comments by the reviewers have helped to improve the manuscript.

Topical Editor J.-P. Duvel thanks D. Thorsen and another referee for their help in evaluating this paper.

## References

- Andrews, D. G., Holton, J. R., and Leovy, C. B., *Middle Atmospheric Dynamics*, Academic Press, 1987.
- Dunkerton, T. J., The role of gravity waves in the quasi-biennial oscillation, *J. Geophys. Res.*, 102, 26, 053–26, 076, 1997.
- Dunkerton, T. J., Wave transience in a compressible atmosphere, Part II: Transient equatorial waves in the quasi-biennial oscillation, *J. Atmos. Sci.*, 38, 298–307, 1981
- Geller, M. A., Shen, W., Zhang, M., and Tan, W.-W., Calculations of the stratospheric quasi-biennial oscillation for time-varying wave forcing, *J. Atmos. Sci.*, 54, 883–894, 1997.
- Holton, J. R. and Lindzen, R. S., An updated theory for the quasi-biennial oscillation of the tropical stratosphere, *J. Atmos. Sci.*, 29, 1076–1080, 1972.
- Holton, J. R., Wave propagation and transport in the middle atmosphere, *Phil. Trans. Roy. Soc. London*, A296, 73–85, 1980.
- Kudeki, E. and Franke, S. J., Statistics of momentum flux estimation, *J. Atmos. Sol.-Terr. Phys.*, 60, 1549–1553, 1998.
- Mayr, H. G., Mengel, J. G., Hines, C. O., Chan, K. L., Arnold, N. F., Reddy, C. A., and Porter, H. S., The gravity wave Doppler spread theory applied in a numerical spectral model of the middle

- atmosphere, 2. Equatorial oscillations, *J. Geophys. Res.*, 102, 26, 093–26, 105, 1997.
- Plumb, R. A., The interaction of two internal waves with the mean-flow: implications for the theory of the quasi-biennial oscillation, *J. Atmos. Sci.*, 34, 1847–1858, 1977.
- Plumb, R. A., The quasi-biennial oscillation, *Dynamics of the Middle Atmosphere*, Ed. Holton, J. R. and Matsuno, T., Terra Publishing Company, Tokyo, 217–251, 1984.
- Sasi, M. N. and Sengupta, K., A model Equatorial Atmosphere over the Indian Zone from 0 to 80 km, *Sci. Rep.*, ISRO:VSSC:SR:19:72, 1979.
- Sasi, M. N., Vijayan, L., Deepa, V., and Krishnamurthy, B. V., Estimation of equatorial wave momentum fluxes using MST radar winds observed at Gadanki (13.5° N, 79.2° E), *J. Atmos. Solar. Terr. Phys.*, 61, 377–384, 1999.
- Sato, K. and Dunkerton, T. J., Estimate of momentum flux associated with equatorial Kelvin and gravity waves, *J. Geophys. Res.*, 102, 26, 274–26, 261, 1997.
- Sato, T., *Radar Principles*, MAP Handbook, (Edited by Fukao, S.), 30, 19–53, SCOSTEP Secr., Urbana, 1989.
- Srinivasan, J. and Smith, G. L., Meridional migration of tropical convergence zones, *J. Appl. Meteor.*, 35, 1189–1202, 1996.
- Wallace, J. M. and Kousky, V. E., On the relation between Kelvin waves and the quasi-biennial oscillation, *J. Meteor. Soc. Japan*, 46, 496–502, 1968.
- Wikle, C. K., Madden, R. A., and Chen, T.-C., Seasonal variation of upper tropospheric and lower stratospheric equatorial waves over the tropical Pacific, *J. Atmos. Sci.*, 54, 1895–1909, 1997.